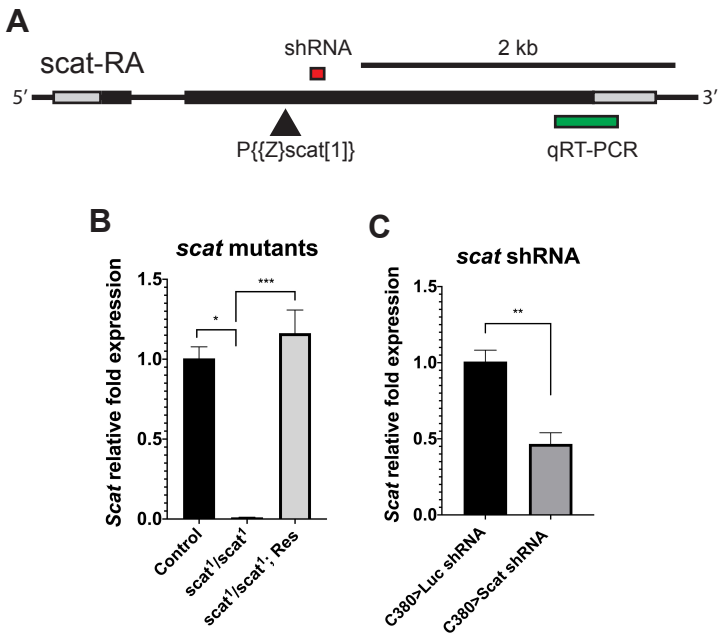

Fig. S1. The *scat*^{1} allele. (A) This is a diagram showing the structure of the *scat* gene in *Drosophila*. Exons are indicated by boxes and the single intron indicated by a line. Gray boxes at the 3' and 5' ends indicate the untranslated regions (UTRs) and black boxes indicate coding sequence. The triangle shows the location of the P-element insertion in the second exon of the *scat* locus. Using an antibody targeting the N-terminal 200 amino acids of the Scat protein, it has previously been shown that this is a null allele (Fari et al., 2016). The region targeted by the *UAS-TRiP(HMS01910)* shRNA line is indicated by the red box. The green box at the 3' end indicates the location of the amplicon analyzed for qRT-PCR. (B) Results of qRT-PCR analysis of *scat* mRNA levels in the larval CNS of controls, *scat*^{1} homozygotes, and the *scat*^{1}*/scat*^{1}*; scat-HA:scat/scat-HA:scat* rescue (Res) lines. *scat* mRNA is reduced in *scat*^{1} homozygotes and restored to near control levels in the rescue line. (C) Results of qRT-PCR analysis of *scat* mRNA levels in control (*C380>Luc shRNA*) and *scat* (*C380>scat shRNA*) larval ventral ganglia. Levels of *scat* mRNA are reduced by at least 50%. Note that this is likely an underrepresentation because *C380-Gal4* drives expression in only a subset of neurons in the ventral ganglion. In both B and C, levels of *scat* transcripts were determined as described in the Methods and then normalized to the control. *N* = 7 ventral ganglia for each genotype. qPCR data shown in B was analyzed by one-way ANOVA followed by a Holm-Sidak multiple comparison test. qPCR data shown in C was analyzed by a two-way Student's t-test. Data are represented as the mean ± SEM for three technical replicates. * $p < 0.05$, ** $p < 0.01$, *** $p < 0.001$.

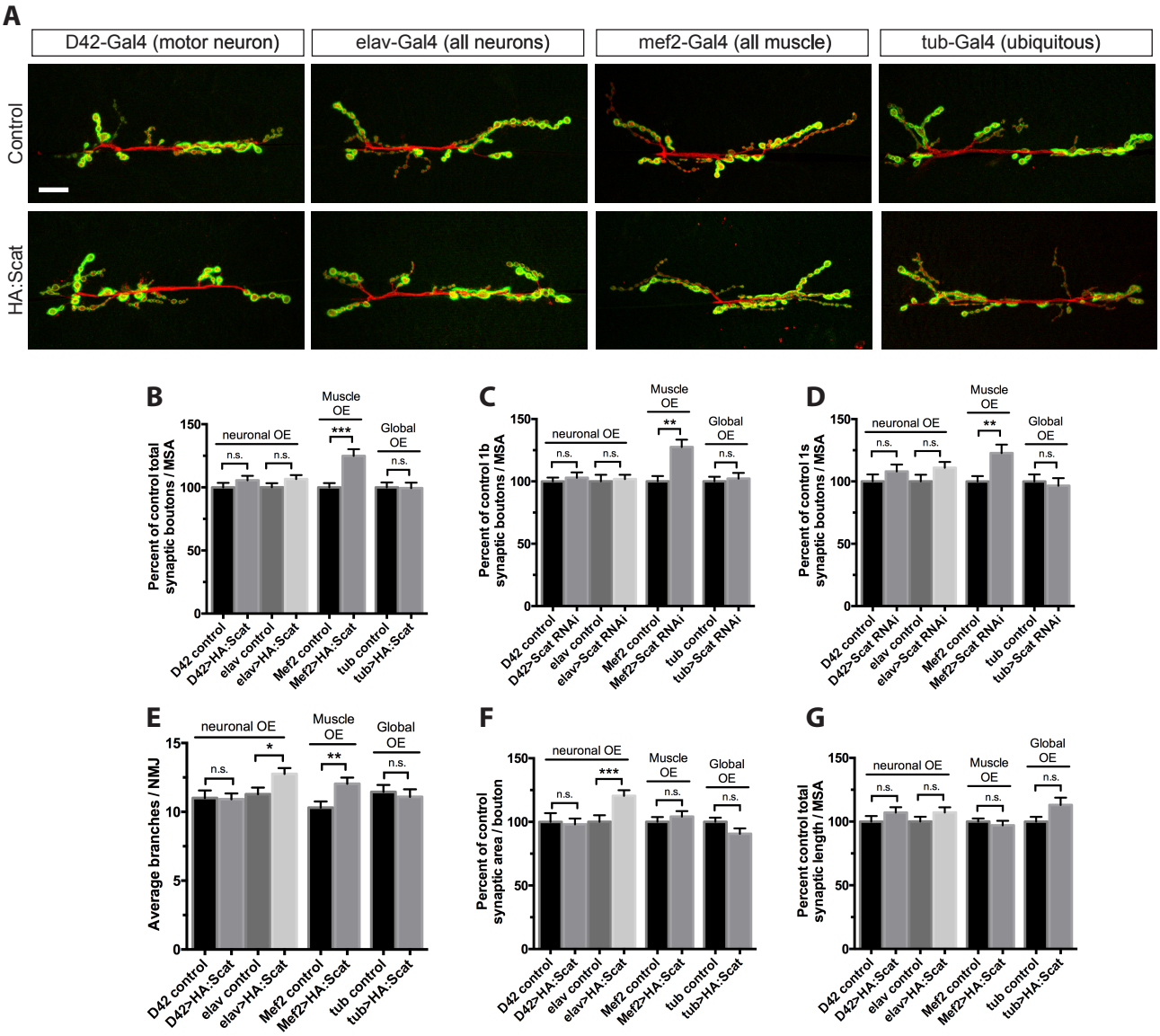

Fig. S2. Overexpression of *scat* has an effect on NMJ development. (A) The inducible *UAS-HA:scat* transgene was expressed using a motor neuron-specific driver (*D42-Gal4*), a strong pan-neuronal driver (*elav-Gal4*), a strong muscle-specific driver (*Mef2-Gal4*), or ubiquitously (*tubulin-Gal4*). NMJs at m6/7 in body segment A3 have been stained with antibodies targeting Dlg (green) and HRP (red). Images show maximum Z-projections. Scale bar, 20 μm. Quantification of the (B) total number of boutons, (C) type 1b boutons, and (D) type 1s boutons shows that bouton number is increased when HA:Scat is overexpressed in larval muscle but not when expressed ubiquitously or in neurons. (E) The number of branches is significantly increased when HA:Scat is strongly expressed in either neurons or muscle. For B-E, $N = 22, 23, 19, 24, 30, 30, 23$, and 23 in the order shown in graphs. (F) Total synaptic area is increased when strongly expressed in muscle. (G)

There is no impact on total synaptic length. Synaptic area and length where quantified using the Morphometrics algorithm. For F and G, *N* = 22, 23, 19, 24, 28, 30, 24, and 27 in the order shown in graphs. All statistical analysis was done by Kruskal-Wallis followed by a Dunn's multiple comparison test. Unless otherwise indicated, all statistical comparisons shown have been compared to driver-specific controls (*driver*/+ heterozygotes). * $p < 0.05$, ** $p < 0.01$, *** $p < 0.001$.

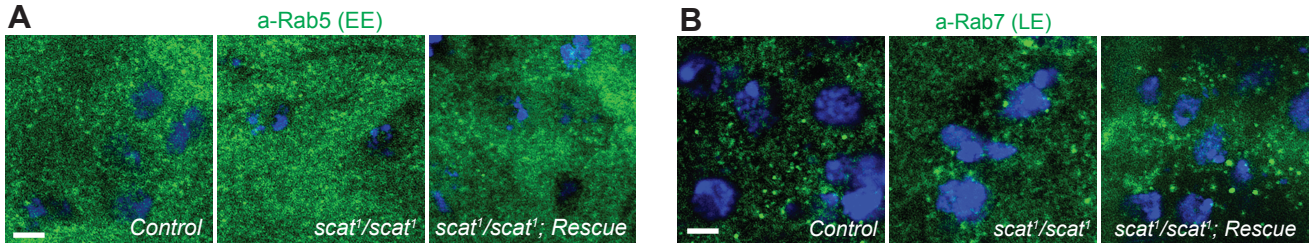

Fig. S3. *scat* mutants do not have defects in Rab5- or Rab7-positive endosomes. Using polyclonal antibodies targeting Rab5 and Rab7 (Hirata et al., 2015), there is no visible defect in the size, number, or distribution of EE or LE in *scat*^{1} mutant MNs. Images shown are single focal planes. Ventral ganglia from wandering third instar larvae from controls, *scat*^{1} homozygotes, and the *scat*^{1}*/scat*^{1}*; scat-HA:scat/scat-HA:scat* rescue lines were stained with antibodies targeting (A) Rab5 or (B) Rab7 (both green). Nuclei are marked by DAPI (blue). Scale bar, 2.5 μm.

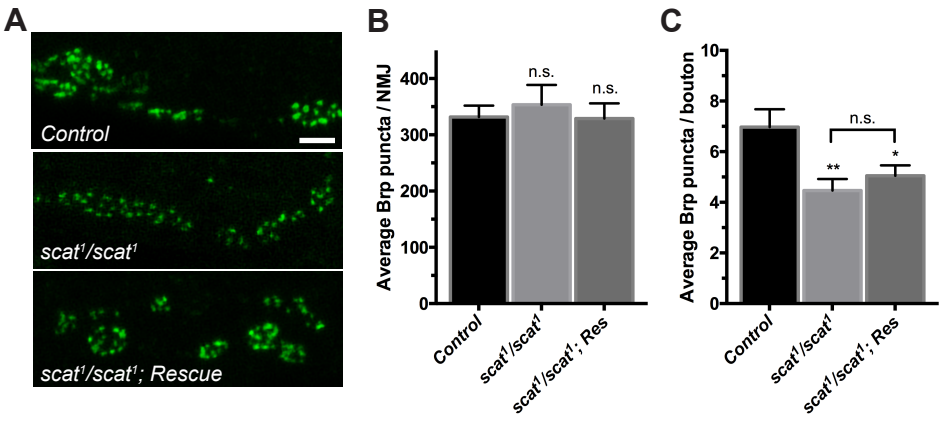

Fig. S4. *scat* mutants do not have active zone defects. A) NMJs innervating muscle 6/7 in body segment A3 from the indicated genotypes stained with an antibody targeting Brp (green). *scat* mutants have an increased number of small boutons with fewer Brp-positive puncta. Scale bar, 5 μm. B) The total number of Brp-positive punctae per NMJ does not change C) The number of Brp-positive punctae per synaptic bouton increases in *scat* mutants. $N = 10$ for each genotype. Statistical analysis was done using a one-way ANOVA followed by a Holm-Sidak multiple comparison test. Data in graphs are represented by the mean ± SEM.

Table S1.

Primer list:

Cloning of *scat* from LD2244 into pUAST (to generate the inducible HA:Scat line)	
Primer pair	Sequence (5' to 3')
Scat_HAf	GATCTTGCGGCCGCATGGCC ACGACAAGATCCGC
Scat_HAr	GGTACCCTCGAGTTAAGCGTAATCTGGAACATCGTA TGGGTAGTAGAGCCAGATCTCCTCCA
Cloning of *scat* from genomic DNA into pCASPR (to generate the genomic rescue line)	
Primer pair	Sequence (5' to 3')
Scat rescue F1	GATCTTGCGGCCGCGTCAGCTGATTTTGCTCAGA
Scat rescue R1	TCAAGCGTAATCTGGAACATCGTATGGGTAGTAGAGCCAGATCTCCTCCA
Scat rescue F2	TACCCATACGATGTTCCAGATTACGCTTGAGCATTCCGAAGTATTCCATA
Scat rescue R2	GGTACCCTCGAGCTTTCACCCCTAAGTTGCAT
Quantitative RT-PCR experiments (for Fig. S1)	
Primer pair	Sequence (5' to 3')
Scat_qPf	ACGAAACTATCGAGCGGGAC
Scat_qPr	TTGAGCTGCCAATCTCTCGG
RpS3_qPf	TCTTTCTTTTCTGCGCACCA
RpS3_qPr	TCGCATTCATTTTGACGTCG